Healing Surface Roughness of Lithographic Nanopatterns through Sub-10 nm Aqueous-dispersible Polymeric Particles with Excellent Dry Etch Durability

Journal:	*Molecular Systems Design & Engineering*
Manuscript ID	ME-ART-02-2018-000007.R1
Article Type:	Paper
Date Submitted by the Author:	16-Apr-2018

Complete List of Authors:	Jiang, Zhen; University of Queensland, Australian Institute for Bioengineering and Nanotechnology Cheng, Hanhao; The University of Queensland, Australian Institute for Bioengineering and Nanotechnology Blakey, Idriss; University of Queensland, Australian Institute for Bioengineering and Nanotechnology Whittaker, Andrew; University of Queensland, Australian Institute for Bioengineering and Nanotechnology

SCHOLARONE™
Manuscripts

Molecular Systems

Design & Engineering

PAPER

Healing Surface Roughness of Lithographic Nanopatterns through Sub-10 nm Aqueous-dispersible Polymeric Particles with Excellent Dry Etch Durability

Received 00th January 20xx,
Accepted 00th January 20xx

DOI: 10.1039/x0xx00000x

www.rsc.org/

Zhen Jiang,[a,d] *Han-Hao Cheng,*[c] *Idriss Blakey*[a,b] *and Andrew K. Whittaker*[a,d*]

The surface roughness in patterned features, commonly termed line-edge roughness (LER), is of particular concern in the manufacture of advanced micro-electronics devices. To address this challenge, we describe an approach whereby the block copolymer poly(oligoethyleneglycol methyl ether methacrylate-*stat*-styrene)-*b*-P(N-[3-(dimethylamino)propyl]methacrylamide) (poly(OEGMA-*stat*-styrene)-*b*-PDMAPMA) is applied to the patterned photoresist, and after thermal annealing reduces significantly the nanoscale surface roughness. The incorporation of hydrophilic OEGMA units enabled the block polymer to be readily dispersed in water and to self-assemble into particles of less than 10 nm in diameter. Importantly, as a result of the incorporation of a relatively high content of the monomer styrene, excellent plasma etch durability was achieved. The relatively low glass transition temperature of the block copolymer allows thermal annealing at temperatures well below the T_g of the photoresist, enabling effective reduction in LER with minimal change to the profiles of the resist sidewalls and trenches. Partial healing of roughness in lithographic patterns with critical dimensions as low as 25 nm was demonstrated. Finally the relatively high aromatic content of the block copolymer allowed the smoothed patterns to be successfully transferred into the underlying silicon wafer.

Design, System, Application

The annealing of surface-coatings of block copolymers (BCPs) has recently been suggested as a means to reduce the line edge roughness (LER) in lithographic nanopatterns. However, the currently-proposed materials self-assemble into large nano-aggregates and have poor resistance to etching, two properties which will prohibit their translation into commercial manufacturing. In this work, we introduce innovative water-dispersible BCP materials, poly(OEGMA-*stat*-styrene)-*b*-PDMAPMA, with sub-10 nm dimensions in solution, and with high resistance to plasma etching. Incorporation of hydrophilic oligoethyleneglycol methyl ether methacrylate units results in formation in stable particles in solution, despite their relatively high styrene content. Importantly, the elevated styrene content affords films of the BCP excellent plasma etch durability. The features of the newly-designed BCPs in smoothing LER include (1) minimal change to the profiles of the resist sidewalls and trenches, (2) demonstrated healing of roughness in high resolution lithographic patterns and (3) smoothed features which can be transferred into the underlying silicon wafer.

Introduction

In recent years advanced nanolithography techniques have been used for microfabrication in a wide range of application areas, including for biomaterials,[1, 2] energy[3, 4] and microelectronics.[5-10] One of the most important applications of nanolithography is in the semiconductor industry. The rapid development of this technology has enabled computers to be present in almost every aspect of our daily life and has revolutionized human society. Despite the impressive achievements made in the field of lithography in recently years, the industry is faced with a number of key challenges before advancing to the next lithographic nodes. One of these challenges, the inherent roughness of printed lithographic features, commonly termed line-edge roughness (LER), has become a key concern for the semiconductor industry.[11] It is known that the roughness of surfaces in fabricated nanopatterns can have deleterious effects on device performance, such as increased optical losses in microfabricated waveguides,[12] off-state leakage and reduced threshold voltage for transistors.[12, 13] Therefore, in order to maintain progress in manufacture of semiconductor devices, the LER should be reduced constantly in line with the scaling nodes set by the semiconductor industry.

[a]*Australian Institute for Bioengineering and Nanotechnology,* [b]*Centre for Advanced Imaging,* [c]*Australian National Fabrication Facility Queensland Node,* [d]*ARC Centre of Excellence in Convergent Bio-Nano Science and Technology, The University of Queensland, St Lucia, 4072, Australia. E-mail: a.whittaker@uq.edu.au*

† Footnotes relating to the title and/or authors should appear here.
Electronic Supplementary Information (ESI) available: [details of any supplementary information available should be included here]. See DOI: 10.1039/x0xx00000x

This journal is © The Royal Society of Chemistry 20xx

In response to this, there has been tremendous effort to develop methods for effectively reducing roughness in nanopatterns.[14-24] Specific targets for roughness have been defined, for example, according to International Technology Roadmap for Semiconductors (ITRS), the LER should be less than 8% of the critical dimension.[11] The first approach to reducing LER is optimization of the resist formulation.[25-27] However, the well-known trade-off between resolution, LER and sensitivity, prohibits reduction of LER without compromising the other critical resist parameters.[28] Methods to reduce LER post-development,[29] such as the use of a thermal hard bake,[15] continuous wave laser heating,[30] plasma treatment[22, 31] and solvent vapour annealing[32] have also been explored in both the academic and industrial communities. Whilst some of these approaches show great promise, they require specialised equipment, and can often result in changes in the critical dimensions and pattern profiles.[15]

An alternative approach introduced by our group exploits the ability of amphiphilic polyelectrolytes[33] to adsorb on surfaces through electrostatic attractions.[34] It was reported that positively-charged polymersomes of amphiphilic polyelectrolytes poly(2-(*N,N*-dimethylamino)ethyl methacrylate)-*b*-poly(*tert*-butyl methacrylate) (PDMAEMA-*b*-PtBMA) could be adsorbed from aqueous solution onto the side walls of patterned resists. A controlled annealing process[34] leads to a significant reduction in the nanoscale roughness of the lithographic patterns. The driving force for the reduction of the roughness, i.e. an increase in smoothness of the patterns, is the reduction in surface energy, i.e. surface area of the polymer-air interface. This approach resulted in smoothing of the roughness of patterned open source photoresists to values of the order of 3.5 nm.

Despite the success of our previously-described approach in reducing LER of photoresists, two significant obstacles to commercial implementation remain. First, the polymers lack etch resistance, due to the lack of aromatic structures and the high oxygen content.[35] Hence transfer of the smoothed LER into the underlying semiconductor devices during the pattern transfer process may not be possible. Second, the amphiphilic block copolymers self-assemble in aqueous media into the form of polymersomes of diameter approximately 20 nm. Particles of this size are clearly incompatible with processes for the sub-30 nm lithographic nodes. Therefore, a new class of polymers is introduced here. The polymers form small particles (< 10 nm) in aqueous solution due to the incorporation of strongly solvating OEGMA units, and have high resistance to plasma etching to allow transfer of the smooth pattern to the underlying substrate, due to the presence of aromatic units.

Our approach to develop the new class of polymeric materials with the targeted properties is to build a block-random copolymer architecture A-*b*-(B-*stat*-C). The incorporation of B units into C block can lead to additional functionality and give further opportunity to tune material properties.[36] The styrene monomer was employed as one of components to offer high etch resistance because of the effective quenching of the electronic energy by the aromatic groups.[37-39] Since the styrene units are hydrophobic and are expected to drive the formation of large aggregates in aqueous solution, a hydrophilic monomeric is incorporated within the B-*stat*-C block to minimise hydrophobic-hydrophobic interactions. To date however, amphiphilic statistical copolymers containing styrene, such as poly(N-alkylacrylamide-*stat*-styrene),[40] poly(N-isopropylacrylamide-*stat*-styrene)[41] and poly(2-(dimethylamino)ethyl methacrylate-*stat*-styrene),[42] were found to be insoluble in water at room temperature except for copolymers with low styrene content (< 8 mol % or 15 wt %). The etch resistance of block copolymer materials with such low styrene content is likely to be severely compromised.[35]

The design of water-dispersible polymers which self-assemble into small aggregates and with a relatively high content of hydrophobic styrene requires that the hydrophilic repeat units be strongly solvated by water so as to effectively shield hydrophobic interactions between styrene units. Most recently, we reported that despite poly(OEGMA-*stat*-styrene)-*b*-PDMAPMA copolymers having a relatively high styrene content,[43] they are readily soluble in water, and capable of forming nanoaggregates of around 15 nm in diameter, as a result of the strong solvating power of OEGMA segments. However, the materials reported previously were relatively large in size (15 nm) and has a high glass transition temperature (98.1 ˚ C). These properties are not suitable for LER reduction in high resolution sub-30 nm lithographic nodes. In the present study, we introduce poly(OEGMA-*stat*-styrene)-*b*-PDMAPMA (Figure 1A) with much lower molecular weight than previously reported[43] and examine its ability to tune the nanoscale roughness. Such polymers are capable of self-assembly into sub-10 nm polymeric assemblies in water, and have excellent plasma etch durability. The polymeric particles could be adsorbed onto the photoresist sidewalls, and following thermal annealing, the LER was significantly reduced. In addition the process led to a minimal change in the CD and the resist sidewall profile, due to the relatively low glass transition temperature of this low molecular weight block copolymer. We demonstrated that the block copolymer was also able to smooth LER in high resolution lithography patterns (CD = 25 nm), and that the smoothed features could be transferred into the underlying silicon wafer.

Experimental

Materials: All chemicals were obtained from Sigma Aldrich and used as received unless otherwise specified. Deionized water was produced by an ELGA Laboratory water station and had a resistivity of 18.2 m/cm. The block copolymers poly(OEGMA-*stat*-styrene)-*b*-PDMAPMA were prepared by reversible addition-fragmentation chain-transfer (RAFT) polymerization using the previously described method.[43]

Preparation of the Aqueous Polymer Solutions: An aqueous solution of poly(OEGMA-*stat*-styrene)-*b*-PDMAPMA at a concentration of 5mg/mL was prepared by directly dissolved in water to form a transparent solution at room temperature

This journal is © The Royal Society of Chemistry 20xx

after being stirred. The pH of the samples was adjusted with dropwise addition of dilute aqueous solutions of HCl or NaOH.

Preparation of Lithographically Patterned Resists: Silicon wafers were treated with acetone and water, followed by O2 plasma cleaning at 200 W for 5 min in the PlasmaPro 80 RIE system. Following this an EUV-sensitive, positive tone photoresist TER60 (4.76 wt % poly[(4-hydroxystyrene)0.6-co-(styrene)0.2-co-(tert-butyl acrylate)0.2], with 0.44 wt % triphenylsulfonium triflate, and 0.076 wt % trioctylamine in ethyl lactate) was spin-coated onto the wafers, followed by annealing at 105 °C on a hot plate for 1 min to give a film with a thickness of 55 nm, determined by spectroscopic ellipsometry. Lithography line and space nanopatterns with different critical dimensions were patterned using an electron-beam lithography (EBL) system field emission scanning electron microscopy (JEOL JEM-7800F or the EUV micro-exposure-tool (MET) from Intel Corp. at doses of 16.7 mJ/cm2. The samples were then baked at 105 ˚C for 60 s on a hot plate followed by development in 2.38% TMAH for 30 s at room temperature, rinsing with deionized water for 15 s and drying with a jet of N2.

Reactive Ion Etching: The RIE was conducted on an Oxford Instruments PlasmaPro 80 RIE etcher with SF6 and CHF3 gases. CHF3 was used as a passivation gas to increase etch anisotropy and SF6 was used as the etching gas. The wafer temperature was kept at 15 ˚C by helium back cooling. Transfer of the pattern to the silicon wafer substrate was performed using an SF6 and CHF3 mixture in RIE mode at a pressure of 15 mTorr at 10 ˚C. The CHF3 flow rate was 35 sccm, and the SF6 flow rate was 20 sccm.

Characterization: Zeta potential measurements of aqueous solutions of polymer were determined by dynamic light scattering and laser Doppler electrophoresis (Zetasizer Nano ZS, Malvern Instruments, Worcestershire, UK). A SurPASS electrokinetic analyzer (Anton Paar) was used for surface zeta potential measurements. XPS measurements were performed using a Kratos Axis ULTRA spectrometer (Kratos Analytical, Manchester, U.K.) with a 165 mm hemispherical electron-energy analyzer and monochromatic AlKα X-ray source (1486.6 eV) operating at 300 W (15 kV, 20 mA). Survey (wide) spectra were acquired using an analyzer pass energy of 160 eV and carried out over a binding energy range of 1200−0 eV with 1.0 eV steps and 100 ms dwell time. High-resolution spectra were acquired at an analyzer pass energy of 20 eV with 0.1 eV steps and 250 ms dwell time, with no charge neutralization. The XPS spectra were analyzed using CasaXPS version 2.3.12 software.

The surface topography of thin films were observed by optical microscopy using 50X or 100X objectives (Olympus BX 60). The thicknesses of the polymer thin films and block copolymers were measured using a Woollam VUV-VASE32 variable angle spectroscopic ellipsometer. Atomic force microscopy (AFM) was performed on a MFP-3D (Asylum research) in tapping mode in air. In order to image the photoresist sidewall profiles, super sharp cantilevers (Nanosensors) with tip radius of 2 nm and nominal resonance frequency in the range of 204 - 497 kHz were used. Nanopatterns with different sizes of line and spaces were imaged using field emission scanning electron microscopy (JEOL JEM-7800F) at an acceleration voltage of 2 kV and a working distance of 3.0 mm in gentle-beam mode. The CD and LER of the patterned features were analyzed using Summit v7.5.1, a commercial lithography metrology software package from EUV Technology (Martinez, CA). The LER values were determined along the full length of the line using a polynomial edge detection algorithm with a threshold value of 0.5 determined by the average line threshold reference, and the associate frequency roughness was expressed as a power spectral density (PSD) function. The SEM image of the etched silicon wafer was taken using an FEI Scios FIB - Dual Beam SEM.

Results and discussion

The design and aqueous solution behaviour of water-soluble block copolymers. The block copolymers were designed to have principal three characteristics: (1) high content of etch resistant repeat units, (2) ready dissolution in aqueous media to form small particles (< 10 nm) and (3) positive charge. To accomplish this, block-random copolymers with A-*b*-(B-*stat*-C) architecture were prepared. The styrene units are expected to impart plasma etch resistance as it is well established that aromatic units are very effective electronic energy quenchers.[39] However, styrene is a hydrophobic monomer and may drive the formation of large aggregates, unsuitable for application in sub-30 nm lithographic features. To achieve a high styrene content and maintain solubility/dispersibility in water, styrene was copolymerized with a hydrophilic monomer so as to shield the hydrophobic interactions. OEGMA has previously been copolymerized with hydrophobic methacrylate monomers to form water dispersible polymers,[44] and is used in this work to prepare blocks containing styrene but with overall hydrophilic characteristics.

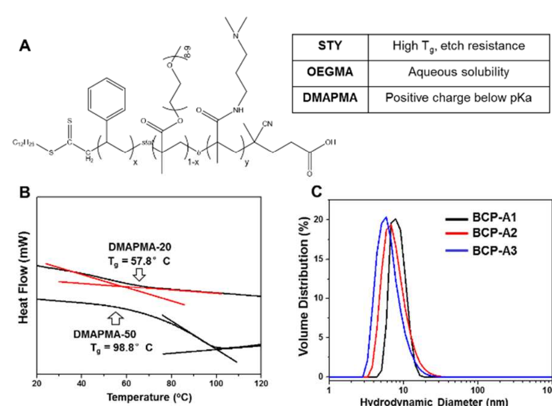

Figure 1. (A) The chemical structure of water-soluble amphiphilic block copolymer poly(OEGMA-*stat*-styrene)-*b*-PDMAPMA (B) DSC thermograms of PDMAPMA blocks with different degrees of polymerization. (C) Volume size distributions of BCP-A1-A3 in aqueous solution measured by DLS.

Please do not adjust margins

In order to facilitate the charged-directed adsorption of the polymeric assemblies onto negatively-charged photoresist sidewalls, the block copolymer should carry a positive charge. This is achieved by extending the poly(OEGMA-*stat*-styrene) block with a block capable of carrying a positive charge. In our previous work we used 2-(*N,N*-dimethylamino)ethyl methacrylate with pKa of 7.6 as the cationic block,[34] however in this study a homopolymer block of DMAPMA was used. DMAPMA has two key advantages over DMAEMA: (1) PDMAPMA has a higher pKa of 9.4,[45] with a measured zeta potential of + 16 mV at pH of 8.3. The high pKa means that the polymer should remain highly charged at relatively high pH, resulting in a broader range of operating conditions. Moreover, resist sidewalls are more negatively-charged at higher pH and therefore stronger interactions between the ionized block copolymer and substrate may result.[34] (2) The higher T_g of PDMAPMA[46] may be used to offset the relatively low T_g of the poly(OEGMA-*stat*-styrene) (-37 °C) block which is a viscous liquid at room temperature. In addition, the incorporation of a "hard" DMAPMA segment with high T_g should result in improved processability for practical applications.

We previously reported the synthesis and aqueous solution behaviour of the poly(OEGMA-*stat*-styrene)-*b*-PDMAPMA.[43] It was reported that the copolymers having high styrene content formed nanoaggregates with diameter of around 15 nm when dispersed into water. However, aggregates of such relatively large size are not suitable for reduction of LER in sub-30 nm lithographic nodes. Moreover, the DMAPMA segment in the block copolymer was reported to have a relatively high T_g of 98.1 ˚C, making it difficult to select appropriate thermal annealing conditions since some photoresists have been reported to have T_g close to this value.[30] Annealing above T_g of the DMAPMA block would potential result in collapse of the lithographic pattern.

In response to these design challenges, we prepared a series of low molecular weight block copolymers BCP-A1-A3 with different styrene contents (Table 1). The glass temperature of the homopolymer PDMAPMA with DP equal to 20 was observed to be 57.8 °C (Figure 1B), significantly lower than that of DMAPMA segment in BCP-A. The block copolymer BCP-A1 exhibits two glass transition temperatures in the DSC traces at -31 °C and 58 °C (Figure S2). In contrast to the high molecular weight counterpart BCP-A which would only be dispersed into water after be magnetically shaken for 15 minutes, BCP-A1 formed a transparent aqueous solution on shaking for ca. 15 s.

Dynamic light scattering was used to determine the size of the copolymers in aqueous solution (Figure 1C).The hydrodynamic diameter of BCP-A1 was found to be 8.0 ± 0.5 nm, significantly smaller than that of BCP-A (14.7 ± 0.7 nm). This was confirmed by ^{1}H diffusion-ordered spectra DOSY NMR, and the diffusion coefficients of BCP-A and BCP-A1 were 2.64 ± 0.05×10^{-11} m^{2}s^{-1} and 4.88 ± 0.04×10^{-11} m^{2}s^{-1}, respectively. The average diameters of the series poly(OEGMA-*stat*-styrene)-*b*-PDMAPMA decreased with decreasing content of styrene, due to the reduced tendency of the copolymer chains to aggregate. Based on these results, the small assemblies of BCP A1-A3, with average hydrodynamic diameters less than 10 nm in aqueous solution, are promising materials for smoothing LER in the sub-30 nm lithographic regime.

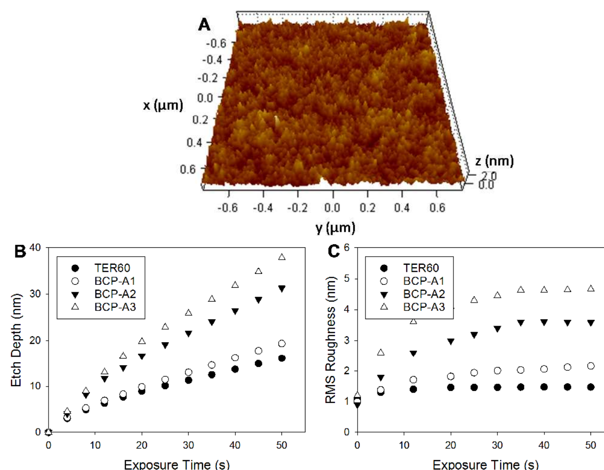

Figure 2. (A) AFM height image of a block copolymer BCP-A1 spin-coated thin film. Plot of block copolymer thin films thickness as determined by ellipsometry (B) and (C) RMS roughness determined by AFM as a function of plasma etching time.

Etch resistance of the block copolymers. In addition to a relatively low T_g and small aggregate size, another essential property of these copolymers is high resistance to plasma etching. Previously it was shown that LER after pattern transfer is related to the durability of the polymer template materials during the transfer process.[35] If the polymeric material is unstable to plasma irradiation, roughness may be produced in the resist sidewalls and be subsequently transferred into the substrate.[47] Likewise, a high etch resistance of the photoresist materials may prevent propagation of roughness into the semiconductor substrate.[48] Therefore, in the current study highly etch resistant styrene units were included within the poly(OEGMA-*stat*-styrene)-*b*-PDMAPMA with the aim to improve the etch resistance and prevent roughness arising from the pattern transfer.

The etch resistance of the films of the block copolymers prepared by spin-coating DMF solutions onto silicon wafer was investigated and compared with the behaviour of TER60, a well-known etch-durable photoresist material. The AFM height image (Figure 2A) demonstrates a smooth initial film of RMS = 1.1 ± 0.4 nm. The high quality film forming behaviour is ascribed to the good solvating power of DMF solvent to both DMAMA[49] and the poly(OEGMA-*stat*-styrene) blocks.

This journal is © The Royal Society of Chemistry 20xx

Table 1. Properties of block copolymers with different compositions

CODE	n_{DMAPMA}:$n_{styrene}$:n_{OEGMA}	[b]$M_{n,theo}$/g.mol^{-1}	[c]Hydrodynamic Diameter/nm	Polydispersity[c] Index (PDI)	[d]Diffusion Coefficient/ $m^2 s^{-1}$	[e]Ohnishi Parameter
BCP-A[a]	50:56:21	23100	14.7 ± 0.3	0.408	2.64 ± 0.05×10^{-11}	3.09
BCP-A1	20:23:7	10230	8.0 ± 0.5	0.332	4.88 ± 0.04×10^{-11}	3.11
BCP-A2	20:23:18	14530	6.8 ± 0.6	0.276	5.64±0.45×10^{-11}	4.01
BCP-A3	20:23:26	18330	5.6 ± 0.2	0.239	6.85±0.23×10^{-11}	4.83

[a] Reported in Reference 43. [b] $M_{n,theo}$ was calculated using the following equation: $M_{n,theo}$ = conv. × [monomer]/[macro-CTA] × Mmonomer + $M_{n,theory}$ of macro-CTA. [c] D_h and PDI of assemblies determined by DLS analysis at 25 °C. [d] Diffusion coefficient and D_h determined by DOSY NMR. [e]Ohnishi parameter was calculated as reported previously.[39]

The change in thin film thickness (etching depth) for the block copolymers as a function of plasma irradiation time was determined by ellipsometry and the results are in Figure 2B. For all of the block copolymers, a high initial rate of loss film thickness was observed and this dropped after about 10 s exposure to a steady rate of etching. This is a characteristic response of a resist material to constant plasma etch conditions, resulting from strong initial plasma-induced modification of the photoresist material properties.[31] Of note, the etch rate of block copolymer BCP-A1 with the lowest OEGMA content was found to be only slight higher than that of the TER60, despite having a higher Ohnishi parameter (3.11 vs. 2.81 for TER60). This is ascribed to effective radiation energy migration and quenching by the phenyl rings, and so the durability of the block copolymer is higher than expected from that estimated using the Ohnishi model.[50] Similar observations have been reported for copolymers of α-methylstyrene and MMA.[50] The block copolymers BCP-A2 and BCP-A3 with much higher OEGMA contents and Ohnishi parameters were observed to be etched faster than BCP-A1. We conclude that the incorporation of higher levels of OEGMA significantly compromises the etch durability of the block copolymers.

The interaction of the plasma with the polymer may itself induce surface roughness; this important property was measured by AFM and the results are shown in Figure 2C. It can be seen that the RMS roughness initially increases rapidly for all polymers and reaches a steady value after approximately 30 s exposure. The development of surface roughness at short exposure times could be a result of removal of oxygen-containing groups and the effective breakdown of the structure of polymer chains at the film surface.[35, 51] The reduction in rate of roughening is likely due to the formation of a more resistant layer by the incident plasma irradiation. The final roughness induced by the exposure to the plasma was in proportion to the content of OEGMA in the copolymers. Based on the above results, the block copolymer BCP-A1 had the most desirable properties and was selected for subsequent studies of healing of LER and pattern transfer of high resolution lithographic features.

Properties of adsorbed block copolymers onto model flat and rough surfaces. The capacity of the positively charged polymeric particles to adhere to the resist sidewalls was initially tested on a model planar surface containing pendant tertiary esters.[34]The tertiary esters were deprotected to form carboxylic acid moieties by exposure UV light irradiation, thus replicating the chemistry, specifically the surface charge, of photoresist sidewalls.[34] The surface charge of the films was measured by streaming potential to be –87 mV at a pH of 8.3. The substrates were then dip-coated into an aqueous solution of the block copolymer at a pH of 8.3, followed by rinsing and drying with Milli-Q water and N_2 to remove the unbound particles. Ellipsometry showed that the thickness of the polymer films before and after dip-coating with block copolymers was 19.3 ± 0.1 nm and 20.8 ± 0.3 nm, respectively. The coating process was further studied using X-ray photoelectron spectroscopy (XPS) and atomic force microscopy (AFM). Figure S1 shows the survey spectrum and high-resolution XPS spectra in the N1s region before and after dip-coating. It is clear that no nitrogen peak can be observed prior to dip-coating, while a small peak at 402 eV is evident after dip-coating, attributed to the nitrogen atoms in the PDMAPMA block. The appearance of the nitrogen signal in XPS and increased thickness confirmed by ellipsometry clearly

Please do not adjust margins

indicated the successful adhesion of the block copolymer to the model flat surface.

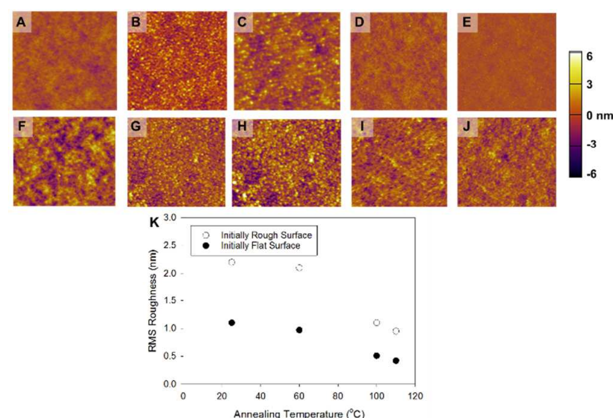

Figure 3. (A-E) AFM images (1.5× 1.5 μm^2) of a negatively-charge model flat surface (A), after coating with block copolymer BCP-A1 (B) and annealing at (C) 60 ˚ C, (D) 85 ˚ C, (E) 110 ˚ C. (F-J) AFM images of a model rough surface (F) and after coating with block copolymer (G) and annealing at (H) 60 ˚ C, (I) 85 ˚ C, (J) 110 ˚ C. (K) The RMS surface-roughness of the films determined after annealing at various temperatures.

The morphology of the model flat surface before and after dip-coating was studied by AFM and the images are shown in Figure 3. The original model flat surface was featureless with a root mean square (RMS) roughness of 0.3± 0.1 nm (Figure 3A). After dip-coating with BCP-A1, adsorbed spherical nanoparticles with high surface coverage could be observed. The average particle diameters and particle heights were measured to be 25-30 nm and 1.2-2.5 nm, respectively indicating that the polymer particles flatten when attached to the flat surface as a result of strong electrostatic interactions.[52] The RMS roughness of the film was found to increase to 1.1 ± 0.2 nm after adsorption of polymer particles.

After attachment of the BCP assemblies, the samples were thermally annealed in vacuum at different temperatures for 5 minutes. An annealing temperature at 60 °C, which is close to the glass transition temperature of the BCP, was initially selected for this study. It was observed that the adsorbed polymer particles flattened more significantly and started to fuse together during thermal annealing (Figure 3C). However, the RMS surface roughness was found to be decreased only by 12% after annealed at this temperature. However, annealing at 85 °C resulted in the complete disappearance of the spherical particulate structure and the RMS surface roughness was found to be significantly reduced to 0.5 ± 0.2 nm (Figure 3D). The reduced surface roughness is due to the rearrangement of the polymer chains upon annealing to adopt a low energy (low surface area) configuration.[33, 34] Further increasing the temperature to 110 °C (Figure 3E) resulted in values of RMS roughness that were not significantly different to that achieved at 85 °C (Figure 3K). These results indicate that the sub-10 nm assemblies have successfully adhered to negatively-charged surfaces and produced smoother surfaces after thermal annealing.

The concept of surface smoothing was subsequently tested with model rough surfaces prepared by the controlled diffusion of a photoacid, which is a model for the roughness produced in features of lithographically patterns.[34] AFM images of the model rough surface (Figure 3F) show an RMS roughness of 1.8 ± 0.3 nm, which is equivalent to approximately 5.4 nm when measured at 3σ. After dip coating, spherical particles were observed on the rough surface (Figure 3G). At this stage, the RMS roughness was measured to be 1.7 ± 0.5 nm, similar to the model rough surface, implying the adsorbed block copolymer particles conformed to the underlying features. The RMS roughness was reduced to 1.5 ± 0.8 nm after thermal annealing at 60 °C for 5 minutes (Figure 3H), consistence with the results for the model flat surface. Further increasing the annealing temperature to 85 °C and 110 °C again resulted in a further reduced RMS roughness of 1.0±0.4 nm (Figure 3I and 3J). As indicated above the reduction in surface roughness is explained as being due to the rearrangement of the polymer chains so as to adopt a smoother surface in order to decrease the overall surface energy.[34]

Healing surface roughness in lithography patterned resist features. The results so far presented confirm that the assemblies of BCP-A1 could adhere to negatively-charged surfaces and that annealing leads to significantly smoother surfaces. The extension of this strategy to healing of roughness in patterned resist features was then explored. The photoresist pattern studied here consisted of 156 nm lines and 70 nm spaces patterned by electron beam lithography. The 3σ LER of the lines was measured to be 8.0 ± 0.8 nm using the SuMMITa software (Figure 4A). To confirm that the annealing step did not alter the CD or LER of the patterns, uncoated EBL patterns were annealed at 85 °C for 5 mins. The average CD after this control annealing was found to be 156 ± 2 nm and 3σ LER equal to 7.9 ± 0.5 nm (Figure 4B), values close to the unannealed patterns. After dip-coating the EBL patterns in an aqueous solution of PCB-A1 and thermal annealing at 85 °C (Figure 4C), the 3σ LER was found to be reduced to 5.6 ± 0.5 nm (28 % reduction in LER). However, it was observed that further annealing at 110 °C resulted in significant reflow or collapse of the patterned photoresist (Figure 4D).

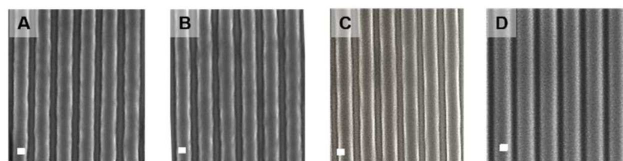

Figure 4. (A) Top-down SEM images of TER60 resist patterned using EBL lithography. (B) Patterned resist annealed at 85 °C as a negative control. Patterned resists after dip-coating with BCP-A1 and annealing at 85 °C (C) and 110 °C (D). All scale bars are 100 nm.

This journal is © The Royal Society of Chemistry 20xx

The average critical dimension (CD) of EBL patterns was measured to be 160 ± 1 nm after polymer coating and annealing at 85 °C, indicating minimal change (less than 5 nm) in CD. Clearly the small size of the polymeric assemblies has minimal impact on the CD of the resist patterns. Such a negligible change in CD after treatment with the block copolymers is highly significant since most processes previously explored to reduce LER have been observed to significantly change the CD and the pattern profile.[15] Such loss of pattern fidelity is not desirable for the subsequent pattern transfer.

The line edge roughness of the EBL patterns was examined using a power spectral density (PSD) analysis, as presented in Figure S3. Because edge roughness is composed of a broad band of spatial frequencies, the PSD analysis can provide more detailed information on the roughness as a function of frequency.[32] From the PSD data depicted in Figure S3, when the EBL patterned wafer was dip-coated with BCP-A1 aqueous solution and underwent annealing, healing of LER was observed over the entire frequency range from 1 μm^{-1} to 500 μm^{-1}. Similar observations were previously reported for polymersomes assembled from amphiphilic copolymers to smooth the LER.[34]

To demonstrate the ability of such 10-nm polymeric particles to reduce LER in high resolution lithography nanopatterns, line-space patterns with CD of 45 nm and 25 nm were printed on EUV resists using an EUVL microexposure tool (Figure 5). As a negative control, the pattern was annealed at 85 °C for 5 minutes, after which the average CD was found to be 46 ± 2 nm and 3σ LER equal to 5.1 ± 0.4 nm (Figure 5 A,D). After dip-coating with BCP-A1 aqueous solution followed by thermal annealing at 85 °C for 5 mins the LER decreased from 5.1 ± 0.4 nm to 3.0 ± 0.3 nm and the average CD was measured to be 49 ± 1 nm. This strategy was also applied to EUVL patterned resist features with CD as small as 25 nm, as shown in Figure 5. The initial LER was found to be 5.2 ± 0.3 nm and was again decreased to 2.7 ± 0.4 nm following dip-coating and thermal annealing. The result demonstrates that the adsorption of the sub-10 nm BCP assemblies into narrow trenches is feasible.

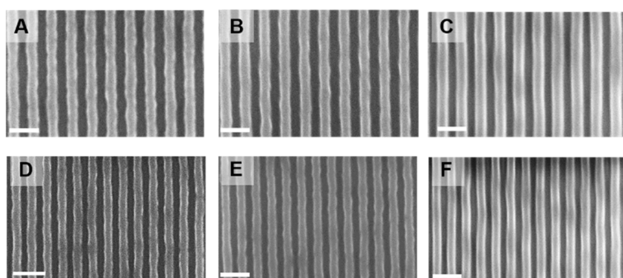

Figure 5. SEM images of TER60 resist patterned using EUV lithography with 45 nm lines and spaces (A, B, C), and 25 nm lines and spaces (D, E, F). Patterned resist annealed at 85 °C (B,E) as a negative control. (C,F) Patterned resists after dip-coating with BCP-A1 and annealing at 85 °C. All scale bars are 100 nm.

In order to further understand the effect of coating of the lithographic features with block copolymer, AFM was used to characterize the resist trench profile before and after coating and annealing (Figure 6). In order to obtain AFM images of the high aspect ratio photoresist profiles,[30] EBL patterns with 320 nm lines and 80 nm spaces were prepared, and a super-sharp AFM tip with a radius of 2 nm was used to assess surface topography of the sidewalls and within the resist trenches. After treatment with BCP-A1 and thermal annealing at 85 °C, the bottom of the trench had not collapsed, in contrast with previous reports in which a hard bake step was used.[15] Notably there is only a negligible change in the trench profile after the LER healing process. The thermal annealing temperature used in our process is much lower than the T_g of the photoresist material. The results also demonstrate the significant flattening of the adsorbed polymer particles on the photoresist sidewall surfaces.

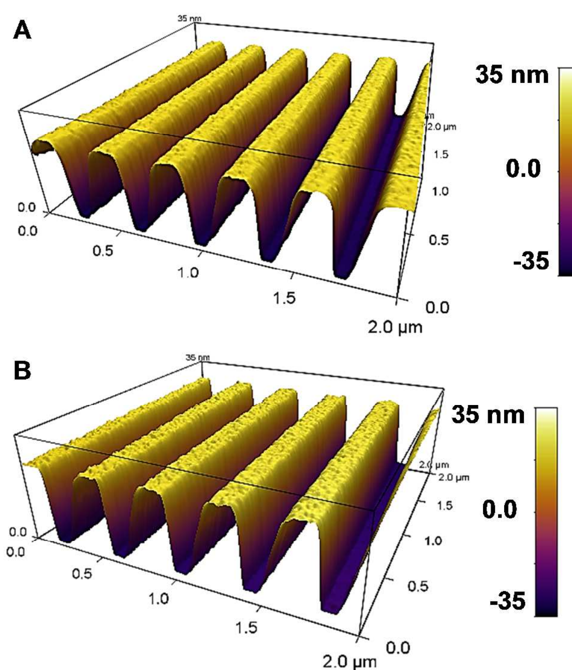

Figure 6. Resist profiles obtained from AFM measurements showing (A) the original TER60 resist patterned by EBL lithography with 320 nm lines and 80 nm spaces, and after dip-coating with BCP-A1 and annealing at 85 °C (B).

This journal is © The Royal Society of Chemistry 20xx

Please do not adjust margins

Pattern transfer of smoothed LER into the silicon substrate. The results presented up to this point demonstrate the ability of the water-soluble block copolymer to smooth the LER in lithographic patterned resists. However, for successful implementation of this LER smoothing strategy for advanced patterning applications, it is essential that the improved LER be etch-transferable to underlying semiconductor substrates.[47, 53-57] Transfer of EBL patterns with 156 nm lines and 70 nm spaces into the Si substrate was performed using a SF_6/ CHF_3 plasma, followed by complete removal of the photoresist using O_2 plasma in order to evaluate the morphology and LER of the etched silicon wafer. Note that the process conditions were not fully optimised however the results here demonstrate the concept of transferring improved LER to the substrate. The tilted cross-section view shows the vertical etched Si profile (Figure S4), demonstrating a successful Si pattern transfer. The LER of the etched silicon wafer was measured to be 7.0 ± 0.2 nm (Figure 7A), which is slightly lower than the original EBL photoresist patterns (7.9 ± 0.5 nm). It is likely that the etch process itself could have slightly beneficial impact on the LER.[31, 35] The PSD analysis indicates that the high roughness frequency component was slightly reduced after pattern transfer, consistent with previous reports (Figure S5).[58] Thermal annealing (Figure 7B) had no appreciable effect on the LER (6.9 ± 0.9 nm). However, the LER of the pattern transferred to the silicon wafer after smoothing by coating with BCP-A1 and annealing was measured to be 5.7 ± 0.5 nm (Figure 7C). The LER of the patterned resist before etch was 5.6 ± 0.5 nm (Figure 4C) indicating that the improved LER was transferred virtually intact and that the smoothed features are etch transferable. Similar observations were reported when using robust polystyrene resists as templates for pattern transfer into silicon wafer.[59]

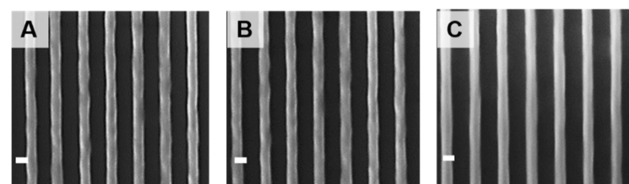

Figure 7. SEM images of silicon substrate after transfer of EBL patterns into silicon wafers: (A) without prior block copolymer treatment; (B) without prior block copolymer treatment and annealed at 85 °C, and (C) treated with BCP-A1 followed by thermal annealing at 85 °C. All scale bars are 100 nm.

Conclusions

We have demonstrated the preparation and achievement of water-soluble block copolymers poly(OEGMA-*stat*-styrene)-*b*-PDMAPMA with the targeted multi-functionalities, for smoothing of roughness of lithographic features. The incorporation of OEGMA and a relatively high content of styrene units enabled the assembly of small size assemblies with diameter of 8 nm in aqueous solution and for the films formed from these materials to be highly resistant to plasma etching. The use of these block copolymers to smooth the LER of lithographic features and to enable pattern transfer was explored. The low glass transition temperature of the DMAPMA segments, below that of the photoresist substrate, enabled much improved healing of LER with minimal change to the resist trench profile. The innovative block copolymer materials could not only smooth LER in high resolution lithography patterns, but also allow transfer of the smoothed LER into the underlying silicon wafer. These results demonstrate the potential for directed self-assembly of water-soluble block copolymers to address the critical challenge of reducing LER of nanoscale features, and has potential to be used to improve pattern fidelity in advanced micro-electronics and functional device fabrication.

Acknowledgements

This work was performed in part at the Queensland node of the Australian National Fabrication Facility (ANFF), at the University of Queensland node of the Australian Microscopy and Microanalysis Research Facility (AMMRF) within the Centre of Microscopy and Microanalysis (CMM). The authors would like to acknowledge funding of the University of Queensland International Postgraduate Research Scholarship scheme, and project funding from the Australian Research Council (LP0989607, LP120100737, DP130103774, DP140103118 and CE140100036) and the Linkage Infrastructure, Equipment and Facilities Scheme (LE0775684, LE110100028, LE110100033, LE140100087, LE160100168, LE170100158). The authors also thank Mr Ao Chen and Ms Eunice Grinan for assistance with SEM images.

Conflicts of interest

There are no conflicts to declare.

References

1. X. Wang, S. Li, C. Yan, P. Liu and J. Ding, *Nano Letters*, 2015, **15**, 1457-1467.
2. S. Park, Y. J. Kang and S. Majd, *Adv. Mater.*, 2015, **27**, 7583-7619.
3. L. Jiang, X. Wang and L. Chi, *Small*, 2011, **7**, 1309-1321.
4. H. G. Yoo, M. Byun, C. K. Jeong and K. J. Lee, *Adv. Mater.*, 2015, **27**, 3982-3998.
5. D. P. Sanders, *Chem. Rev.*, 2010, **110**, 321-360.
6. D. Bratton, D. Yang, J. Dai and C. K. Ober, *Polym. Adv. Technol.*,

This journal is © The Royal Society of Chemistry 20xx

2006, **17**, 94.
7. A. S. Gangnaik, Y. M. Georgiev and J. D. Holmes, *Chem. Mater.*, 2017, **29**, 1898-1917.
8. S.-J. Jeong, J. Y. Kim, B. H. Kim, H.-S. Moon and S. O. Kim, *Mater. Today*, 2013, **16**, 468-476.
9. H. S. Moon, J. Y. Kim, H. M. Jin, W. J. Lee, H. J. Choi, J. H. Mun, Y. J. Choi, S. K. Cha, S. H. Kwon and S. O. Kim, *Adv. Funct. Mater.*, 2014, **24**, 4343-4348.
10. H. M. Jin, D. Y. Park, S. J. Jeong, G. Y. Lee, J. Y. Kim, J. H. Mun, S. K. Cha, J. Lim, J. S. Kim and K. H. Kim, *Adv. Mater.*, 2017, DOI: 10.1002/adma.201700595.
11. Semiconductor Industry Association, International Technology Roadmap for Semicondutor, Washington, DC, USA, 2013, www. itrs2. net.
12. L. Persano, A. Camposeo and D. Pisignano, *J. Mater. Chem. C*, 2013, **1**, 7663–7680.
13. C. H. T. Diaz, H.; Ku, Y.; Yen, A.; Young, K. An, *IEEE Electron. Device Lett.*, 2001, **22**, 287−289.
14. J. L. Sturtevant, J. E. Meiring, T. B. Michaelson, A. T. Jamieson, G. M. Schmid and C. G. Willson, *Proc. SPIE*, 2005, **5753**, 350-360.
15. J. L. Sturtevant, M. Padmanaban, D. Rentkiewicz, S. Lee, C. Hong, D. Lee, D. Rahman, R. Sakamuri and R. R. Dammel, *Proc. SPIE*, 2005, **5753**, 862-869.
16. Q. Lin, Y. Inatomi, T. Kawasaki and M. Iwashita, *Proc. SPIE*, 2006, **6153**, 61533X-61531.
17. Q. Lin, P. Zhang, J. M. Jaramillo, S. Cassel, T. Wallow, A. Acheta, A. R. Pawloski, S. Bell and R. H. Kim, *Proc. SPIE*, 2006, **6153**, 61533Y-61531.
18. M. Chandhok, K. Frasure, E. S. Putna, T. R. Younkin, W. Rachmady, U. Shah and W. Yueh, *J. Vac. Sci. Technol., B* 2008, **26**, 2265-2270.
19. E. Pargon, M. Martin, K. Menguelti, L. Azarnouche, J. Foucher and O. Joubert, *Appl. Phys. Lett.* , 2009, **94**, 103111-103113.
20. R. D. Allen, S. Kobayashi, S. Shimura, T. Kawasaki, K. Nafus, S. Hatakeyama, H. Shite, E. Nishimura, M. Kushibiki, A. Hara, R. Gronheid, A. Vaglio-Pret and J. Kitano, *Proc. SPIE*, 2010, **7639**, 763914-763911.
21. C. R. M. Struck, R. Flauta, M. J. Neumann, K. N. Kim, R. Raju, R. L. Bristol and D. N. Ruzic, *J Micromech. Microeng.*, 2010, **20**, 075038.
22. L. Azarnouche, E. Pargon, K. Menguelti, M. Fouchier, O. Joubert, P. Gouraud and C. Verove, *J. Vac. Sci. Technol., B* 2013, **31**, 012205-012201.
23. J. M. Kim, Y. H. Hur, J. W. Jeong, T. W. Nam, J. H. Lee, K. Jeon, Y. Kim and Y. S. Jung, *Chem. Mater.*, 2016, **28**, 5680-5688.
24. K. S. Lee, J. Lee, J. Kwak, H. C. Moon and J. K. Kim, *ACS Appl Mater Interfaces*, 2017, **9**, 31245–31251.
25. J. L. Sturtevant, T. B. Michaelson, A. T. Jamieson, A. R. Pawloski, J. Byers, A. Acheta and C. G. Willson, *Proc. SPIE*, 2004, **5376**, 1282-1293.
26. C. L. Henderson, B. Rathsack, K. Nafus, S. Hatakeyama, Y. Kuwahara, J. Kitano, R. Gronheid and A. Vaglio Pret, *Proc. SPIE*, 2009, **7273**, 727347-727341.
27. T. I. Wallow, C. K. Hohle, J. Jiang, M. O. Thompson and C. K. Ober, *Proc. SPIE*, 2014, **9051**, 90510H-90511.
28. T. Itani and T. Kozawa, *Jpn. J. Appl. Phys., Part 1*, 2013, **52**, 010002-010012.
29. C. A. Mack, *J. Micro/Nanolith. MEMS MOEMS*, 2015, **14**, 033503-033501.
30. B. Jung, C. K. Ober and M. O. Thompson, *J. Mater. Chem. C*, 2014, **2**, 9115-9121.
31. L. Azarnouche, E. Pargon, K. Menguelti, M. Fouchier, M. Brihoum, R. Ramos, O. Joubert, P. Gouraud and C. Verove, *J. Micro/Nanolith. MEMS MOEMS*, 2013, **12**, 041304-041307.
32. A. Vaglio Pret, *J. Micro/Nanolith. MEMS MOEMS*, 2010, **9**, 041203-041207.
33. E. H. H. Wong, M. P. van Koeverden, E. Nam, S. N. Guntari, S. H. Wibowo, A. Blencowe, F. Caruso and G. G. Qiao, *Macromolecules*, 2013, **46**, 7789-7796.
34. Y.-M. Chuang, K. S. Jack, H.-H. Cheng, A. K. Whittaker and I. Blakey, *Adv. Funct. Mater.* , 2013, **23**, 173-183.
35. G. S. Oehrlein, R. J. Phaneuf and D. B. Graves, *J. Vac. Sci. Technol., B* 2011, **29**, 010801-010801.
36. C. Tsitsilianis, G. Gotzamanis and Z. Iatridi, *Eur. Polym. J.* , 2011, **47**, 497-510.
37. S. Imamura, *J. Electrochem. Soc.* , 1979, **126**, 1628-1630.
38. K. Harada, *J. Appl. Polym. Sci.* , 1981, **26**, 3395-3408.
39. H. Gokan, S. Esho and Y. Ohnishi, *J. Electrochem. Soc.* , 1983, **130**, 143-146.
40. M. Nichifor and X. X. Zhu, *Polymer*, 2003, **44**, 3053-3060.
41. C. K. Chee, S. Rimmer, D. A. Shaw, I. Soutar and L. Swanson, *Macromolecules*, 2001, **34**, 7544-7549.
42. C. Zhang and M. Maric, *Polymers*, 2011, **3**, 1398.
43. Z. Jiang, I. Blakey and A. K. Whittaker, , *Poly. Chem.*, 2017, **8**, 4114-4123
44. Z.-Y. Qiao, F.-S. Du, R. Zhang, D.-H. Liang and Z.-C. Li, *Macromolecules*, 2010, **43**, 6485-6494.
45. D. B. Thomas, B. S. Sumerlin, A. B. Lowe and C. L. McCormick, *Macromolecules*, 2003, **36**, 1436-1439.
46. S. Schmitz and H. Ritter, *Macromol. Rapid Commun.* , 2007, **28**, 2080-2083.
47. Y. Hsu, *J. Vac. Sci. Technol., B* 1998, **16**, 3344-3348.
48. D. L. Goldfarb, A. P. Mahorowala, G. M. Gallatin, K. E. Petrillo, K. Temple, M. Angelopoulos, S. Rasgon, H. H. Sawin, S. D. Allen and M. C. Lawson, *J. Vac. Sci. Technol., B* 2004, **22**, 647-653.
49. H. Y. Tian, J. J. Yan, D. Wang, C. Gu, Y. Z. You and X. S. Chen, *Macromol. Rapid Commun.* , 2011, **32**, 660-664.
50. N. Ueno, K. Sugita, S. Sasaki and S. Nagata, *J. Appl. Polym. Sci.*, 1987, **34**, 1677-1691.
51. S. Engelmann, R. L. Bruce, T. Kwon, R. Phaneuf, G. S. Oehrlein, Y. C. Bae, C. Andes, D. Graves, D. Nest, E. A. Hudson, P. Lazzeri, E. Iacob and M. Anderle, *J. Vac. Sci. Technol., B* 2007, **25**, 1353-1368.
52. G. B. Webber, E. J. Wanless, S. P. Armes, F. L. Baines and S. Biggs, *Langmuir*, 2001, **17**, 5551-5561.
53. A. Yahata, S. Urano and T. Inoue, *Jpn. J. Appl. Phys., Part 1*, 1997, **36**, 6722-6723.
54. L. H. A. Leunissen, R. Jonckheere, K. Ronse and G. B. Derksen, *J. Vac. Sci. Technol., B* 2003, **21**, 3140-3143.
55. Q. Lin, A. R. Pawloski, A. Acheta, S. Bell, B. La Fontaine, T. Wallow and H. J. Levinson, *Proc. SPIE*, 2006, **6153**, 615318-615311.
56. M. Fouchier and E. Pargon, *J. Micro/Nanolith. MEMS MOEMS*, 2013, **12**, 041308-041308.
57. E. Pargon, M. Martin, J. Thiault, O. Joubert, J. Foucher and T. Lill, *J. Vac. Sci. Technol., B* 2008, **26**, 1011-1020.
58. T. Y. Ma, P. Xie, L. Godet, P. M. Martin, C. S. Campbell, J. Xue, L. Miao, Y. Chen, H. Dai and C. Bencher, 2013. *Proc. SPIE*, 2013, **8682**, 868206-1.
59. R. A. Farrell, N. Petkov, M. T. Shaw, V. Djara, J. D. Holmes and M. A. Morris, *Macromolecules*, 2010, **43**, 8651-8655.

Toc Graphic and text:

Herein we demonstrate the design and use of sub-10 nm etch-durable polymeric particles for healing roughness in lithographic patterns.

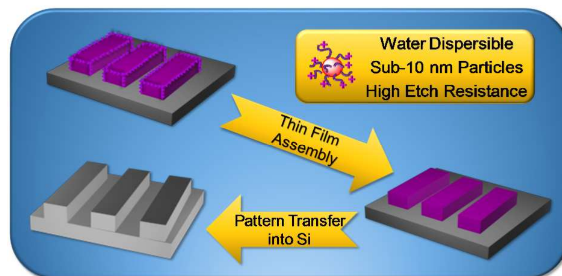

 This journal is © The Royal Society of Chemistry 20xx